Robustness of Topologically Protected Surface States in Layering of Bi_2Te_3 Thin Films

Kyungwha Park, J. J. Heremans, V. W. Scarola, and Djordje Minic
Department of Physics, Virginia Tech, Blacksburg, Virginia 24061, USA
(Received 19 May 2010; published 27 October 2010)

Bulk Bi_2Te_3 is known to be a topological insulator. We investigate surface states of $Bi_2Te_3(111)$ thin films of one to six quintuple layers using density-functional theory including spin-orbit coupling. We construct a method to identify topologically protected surface states of thin film topological insulators. Applying this method to Bi_2Te_3 thin films, we find that the topological nature of the surface states remains robust with the film thickness and that the films of three or more quintuple layers have topologically nontrivial surface states, which agrees with experiments.

DOI: 10.1103/PhysRevLett.105.186801 PACS numbers: 73.20.At, 71.20.Nr, 71.15.Mb

Recently, topological insulators (TIs) with time-reversal symmetry have attracted attention due to their topologically protected states [1–4]. In three dimensions (3D), TIs differ from band insulators in that a bulk energy gap opens due to strong spin-orbit coupling (SOC) with metallic surface states in the bulk energy gap. Several bulk bismuth-based alloys were discovered to be 3D TIs [2–10]. Unlike fragile surface states in ordinary metals, the surface states of TIs are topologically protected in that impurities preserving time-reversal symmetry can neither destroy nor impact the topological nature of the surface states. 3D TIs are classified according to a topological invariant, the Z_2 invariant ν_0 [1]. Strong (weak) TIs have $\nu_0 = 1$ ($\nu_0 = 0$). Recent first-principles calculations [5,11] show that bulk Bi_2Te_3, Bi_2Se_3, and Sb_2Te_3 are strong TIs with a single Dirac cone below the Fermi level, E_F, at Γ ($\vec{k} = \vec{0}$). This feature was confirmed by angle-resolved photoemission spectra (ARPES) [4,7–9].

Thin films offer valuable probes of TIs as well as potential device applications. For example, thin TI films were proposed to be efficient thermoelectric devices that exploit the interaction between top and bottom surface states [12]. Thin films also have considerable advantages in a direct measurement of transport properties of the surface states by emphasizing surface states over bulk states [13]. Very recently, Bi_2Te_3 and Bi_2Se_3 thin films with a thickness of a few nm were fabricated on substrates [14–17] or suspended across trenches [18]. Topological properties of such films have been examined [15–17,19–21]. One theory suggests that the quantum spin Hall phase of a thin TI film oscillates between topologically trivial ($\nu_0 = 0$) and nontrivial ($\nu_0 = 1$) edge states with the film thickness [19]. Another study implies a topological quantum phase transition with an oscillation in an energy gap Δ with the thickness [21]. However, observed ARPES [15–17] on thin films did not show any oscillation in either ν_0 or Δ with thickness. These discrepancies cast doubt on the robustness of topological properties and how to identify them for thin films.

In this work, we treat thin TI films as 3D and construct a method to identify their surface states and determine the topological nature of the surface states. This differs from previous studies [19–21] where thin films were considered to be two dimensional (2D) and focused on topological edge states. Our method is entirely based on density-functional theory (DFT) with SOC (without a model Hamiltonian). The surface states are identified from band structures of slabs, using wave function projections and the decay length of the surface states. Their topological properties are determined by counting the number of crossings of the surface states between time-reversal invariant momenta [1]. As an example, we apply this method to Bi_2Te_3 thin films at six different thicknesses. We show that the topological nature of the surface states remains *robust* with the film thickness and that the surface states are topologically nontrivial ($\nu_0 = 1$) for films three or more quintuple layers (QLs) thick. Our findings are consistent with recent experiments on thin films [15–17].

We begin with a review of the bulk properties of Bi_2Te_3 [22]. A unit cell of bulk Bi_2Te_3 consists of a rhombohedral structure with five inequivalent atoms: two Bi and three Te. For the lattice constants ($a = 4.386$ Å and $c = 30.497$ Å) and the positions of the five atoms, we use experimental data [23]. We calculate the electronic structure of bulk Bi_2Te_3 using a DFT code, VASP [24], within the Perdew-Burke-Ernzerhopf (PBE) generalized-gradient approximation (GGA) [25]. Projector-augmented-wave (PAW) pseudopotentials are used [26]. Plane waves with a kinetic energy cutoff E_c of 175 eV are used as basis sets and 146 irreducible k points ($N_k = 146$) are sampled. Figure 1 shows the bulk band structure computed without and with SOC at time-reversal invariant momenta, Γ, Z, F, and L, with $E_F = 0$. At the Dirac point (Γ), SOC inverts the conduction and valence bands with opposite parities [5].

Let us discuss the structure of a $Bi_2Te_3(111)$ film and parameter values for band-structure calculations of the films. Along the (111) direction (trigonal axis), a Bi_2Te_3 slab is built in units of a QL, which consists of two Bi and three Te layers that alternate [inset in Fig. 2(b)]. In each atomic layer, the Bi or Te atoms form a triangular lattice, and their in-plane positions coincide with those in a (111)

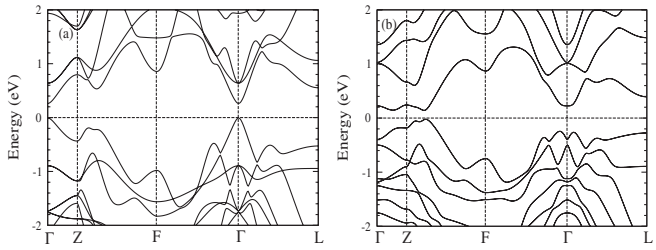

FIG. 1. Band structure of bulk Bi_2Te_3 (a) without SOC and (b) with SOC at symmetry points Γ, Z, F, and L.

surface of a faced-centered-cubic lattice. Neighboring QLs are separated by z_3 ($> z_2 > z_1$), which causes the Te(1) layers between neighboring QLs to interact via weak van der Waals forces, allowing exfoliation [18]. For the slab electronic structure, we use VASP [24] with the PBE GGA and PAW pseudopotentials as in the bulk case. We do not perform reconstruction of the surfaces, as changes due to surface relaxation in the Bi_2Te_3 films appear negligible. When relaxing interlayer separations for a 3-QL slab using VASP, we find that the interlayer separations change less than 3% of the bulk experimental values [23] or at most about 4% of the bulk GGA-optimized values [27]. A lack of reconstruction agrees with experiments performed on films on substrates [28] and with experiments on bulk samples [29], and is supported by the fact that the weak inter-QL binding allows for clean exfoliation of Bi_2Te_3. We also confirm that this small change does not affect the topological nature of the surface states. Compared to the bulk case, the electronic structure of the slabs, especially of surface bands, converges more slowly with parameter values (E_c, N_k, and the number of vacuum layers). For the six slabs with different thicknesses considered, a large vacuum layer equivalent to 5 QLs is added.

Self-consistent DFT calculations with SOC are first carried out using the parameter values listed in Table I until the total energy converges to within 1 μeV. The 2D band structure is then computed non-self-consistently using a charge density distribution obtained from the previous self-consistent calculations. Accuracy in the structure of the surface bands depends on the accuracy in the charge density distribution. Thus, extremely well-converged self-consistent calculations are required for an accurate identification of the surface bands. A relativistic layer-Korringa-Kohn-Rostoker approach can be also used for calculations of surface states [30].

We now introduce our method to identify surface states from the slab band structure. Surface bands refer to bands localized on the top or bottom surface layers of a slab [31]. Thus, not all bands in a slab belong to the surface bands. To identify surface bands, a wave function at a given energy band and $\vec{k}_{\parallel}$ (momentum parallel to the surface) is

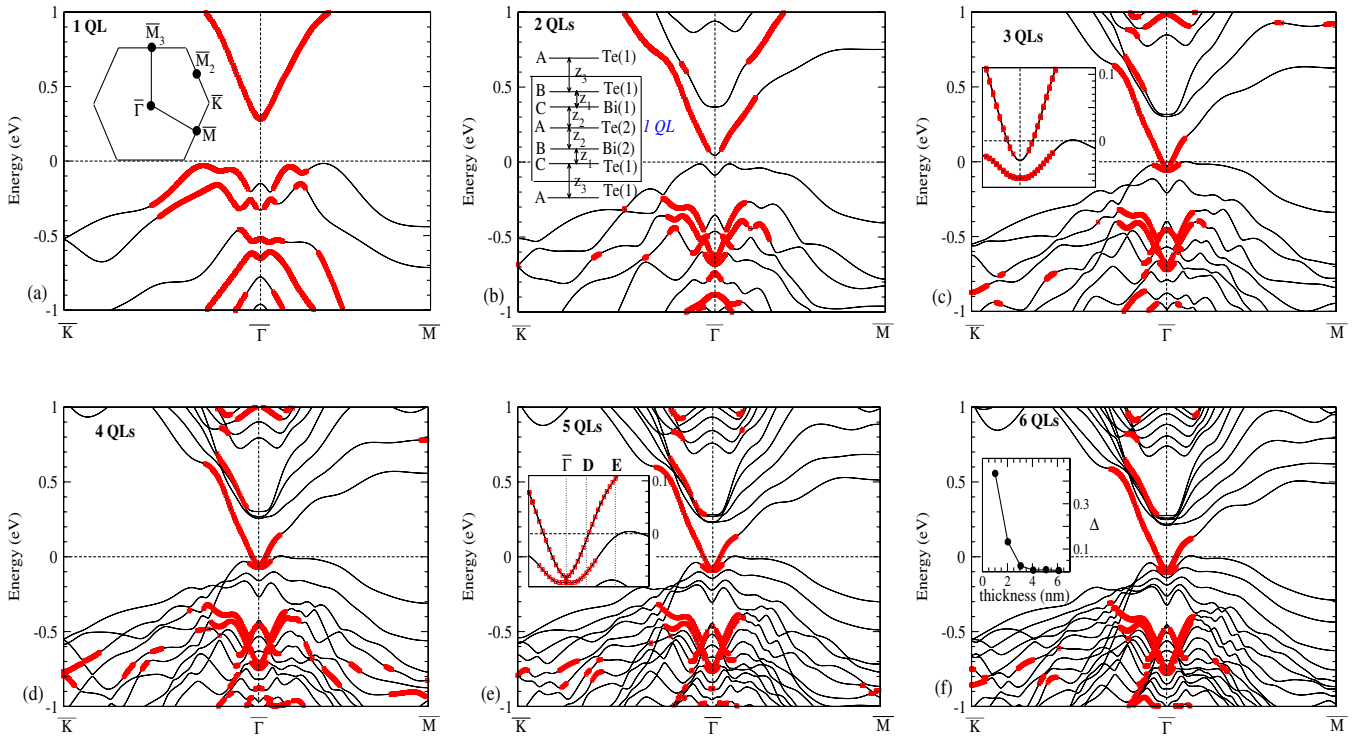

FIG. 2 (color online). Band structures of Bi_2Te_3(111) films with six thicknesses (surface states marked by the squares). Inset in (a) 2D Brillouin zone. Inset in (b) Schematic view of one QL of a Bi_2Te_3(111) film. A, B, and C indicate the planar sites of the Te and Bi atoms. $z_1 = 1.737$ Å, $z_2 = 2.033$ Å, $z_3 = 2.625$ Å [23]. Inset in (c) Zoom-in of the 3-QL band structure near $E_F = 0$. Inset in (e) Zoom-in of the 5-QL band structure near $E_F = 0$. Inset in (f) Δ (eV) vs thickness (nm).

TABLE I. The number of crossings N_c of the surface states across E_F, the energy gap Δ at $\bar{\Gamma}$, and the indirect band gap ΔE_{ind} (eV) as a function of slab thickness (nm).

No. of QLs	Thickness	E_c	N_k	Δ (eV)	N_c	ΔE_{ind}
1	1.0166	300	48	0.4338	0	0.301
2	2.0332	300	96	0.1319	0	0.057
3	3.0497	500	341	0.0261	1	No gap
4	4.0663	500	341	0.0070	1	No gap
5	5.0829	500	341	0.0090	1	No gap
6	6.0993	500	341	0.0055	1	No gap

projected onto spherical harmonics which are nonzero within some radius around each ion [32]. Then two criteria are applied to the wave function projections. In criterion 1, the surface bands are identified based on a critical percentage of the projections onto the top two or the bottom two atomic layers. Criterion 1 is commonly used in various materials [31–33]. In criterion 2, the surface bands are identified according to a critical percentage of the projections onto the topmost or the bottommost QL. Criterion 2 is unique for materials with QL structures and suitable for multiple QL slabs. Our calculated density of states (DOS) supports criterion 2. For the topmost or bottommost QL, the DOS projected onto the Te(1) layer situated at the surface, more closely resembles that projected onto the Te(1) layer below the surface, than that onto the middle Te(2) layer [inset in Fig. 2(b)]. This fact again bolsters the observation that inter-QL binding is weaker than intra-QL binding. Additionally, the electron density spreads over all five atomic layers within the topmost or bottommost QL.

Band structures of $Bi_2Te_3(111)$ slabs of 1–6 QLs, are shown in Fig. 2 with the pure surface bands or states marked. Here the unmarked states correspond to either surface resonant states or bulklike states. The pure surface states are identified by applying criterion 1 to the 1–2-QL slabs and criterion 2 to the other slabs. Critical percentages are initially determined considering the decay length of the surface states, and they are fine-tuned such that the surface states identified within the energy window do not change much with the variation of the critical percentages. The specific critical percentages are as follows: 45% and 30% for 1 and 2 QLs, respectively, and 60%, 50%, 40%, and 40% for 3, 4, 5, and 6 QLs, respectively. We find the decay length of the surface states to be about 2 nm (further discussion follows). Thus, for example, for the 4-QL slab, 50% of the slab contributes to the surface states. For very thin slabs (1–2 QLs), criterion 2 is not applied.

Now we present a physical interpretation of the surface states identified above. Let us first consider a very thick slab where the top surface bands do not interact with the bottom surface bands. When the thick slab has symmetric surfaces (the top and bottom surfaces in an identical environment), the surface bands become fourfold degenerate at $\bar{\Gamma}$, because of Kramers degeneracy at the time-reversal invariant momentum for both the top and bottom surfaces. Away from $\bar{\Gamma}$, the fourfold degeneracy is lifted to a twofold degeneracy due to SOC. Neglecting the fact that the spin-up and spin-down states are not eigenstates in the presence of SOC, for a symmetric thick slab, the top surface bands with spin-up (spin-down) are degenerate with the bottom surface bands with spin-down (spin-up).

As the slab thickness decreases, the top surface bands interact with the bottom surface bands, resulting in an opening of a band gap Δ, even at $\bar{\Gamma}$. At $\bar{\Gamma}$, a linear even combination of the top spin-up and the bottom spin-up surface states are degenerate with a linear even combination of the top spin-down and the bottom spin-down surface states. At $\bar{\Gamma}$, the energies of these even combinations are separated from those of the similar odd combinations (with a double degeneracy) by Δ. This gap increases with increasing $k_{\|}$. As the thickness decreases, Δ increases. Even though the symmetric slab still possesses time-reversal and spatial inversion symmetry, a strong interaction between the top and bottom surfaces mixes spin-up with spin-down states, resulting in a reduction in spin polarization at each surface.

Our calculated values of Δ at $\bar{\Gamma}$ and of an indirect band gap ΔE_{ind} corroborate robust surface states for three or more QLs. The 1 and 2-QL slabs show Δ of 0.4338 and 0.1319 eV at $\bar{\Gamma}$, respectively. This gap decreases exponentially with increasing thickness and it saturates at a thickness of 4 QLs [Table I, inset in Fig. 2(f)], in agreement with Refs. [16,19]. For the 1–2-QL slabs, Δ does not originate entirely from the surface states but surface resonant states are involved. At $\bar{\Gamma}$, for the 1–2-QL slabs, the valence band does not have a surface character [Figs. 2(a) and 2(b)]. The 1 and 2-QL slabs show ΔE_{ind} of 0.301 and 0.057 eV, respectively. As the thickness increases, ΔE_{ind} vanishes.

We now use our accurate identification of surface states in the slabs to examine their topological properties. For a bulk TI, ν_0 is determined from the bulk band structure by a product of parity eigenvalues of all occupied bands (counting Kramers degenerate pairs only once) at the eight time-reversal invariant momenta [1]. However, this procedure is not well defined in a slab where bulklike states can be easily mixed with surface states. Thus, instead, considering a slab to be 3D, we use an equivalent criterion [1]: the surface bands of a TI cross E_F an odd number of times between time-reversal invariant momenta ($\nu_0 = 1$). With the notation in Ref. [1], ν_0 can be obtained from $(-1)^{\nu_0} = \pi_{\bar{\Gamma}}\pi_{\bar{M}}\pi_{\bar{M}_2}\pi_{\bar{M}_3}$, where $\bar{\Gamma}$, $\bar{M}$, $\bar{M}_2$, and $\bar{M}_3$ are four time-reversal invariant momenta in the 2D Brillouin zone [inset in Fig. 2(a)]. If the surface bands cross E_F an odd (even) number of times between $\bar{\Gamma}$ and $\bar{M}$, then $\pi_{\bar{\Gamma}}\pi_{\bar{M}} = -1$ $(+1)$. Here we count only pure surface states not surface resonant states at the point of their crossing E_F, as discussed in Refs. [2,6].

For the 1–2-QL slabs, the surface states neither cross E_F between $\bar{\Gamma}$ and $\bar{M}$ [Figs. 2(a) and 2(b)] nor between $\bar{M}_2$ and

TABLE II. Wave function projections onto each QL (from the topmost to the bottommost QL) for the 5-QL slab, as a function of energy band and $k_{\|}$. The specific $k_{\|}$ points for the v-shaped (U-shaped) band shown in the inset of Fig. 2(e) are labeled as $\bar{\Gamma}_{\mathsf{v}}$, D_{v}, E_{v} ($\bar{\Gamma}_{\mathsf{U}}$, D_{U}, E_{U}). Each band has a double degeneracy. Two wave functions corresponding to $\bar{\Gamma}_{\mathsf{v}}$ have the following projections onto each QL with the opposite spin moments: (0.503, 0.204,0.024,0.085,0.189), (0.189,0.085,0.024,0.204,0.503).

	$\bar{\Gamma}_{\mathsf{U}}$	$\bar{\Gamma}_{\mathsf{v}}$	D_{U}	D_{v}	E_{U}	E_{v}
$k_{\|}$ $(2\pi/a)$	0	0	0.022	0.022	0.057	0.057
Topmost	0.438	0.503	0.490	0.795	0.328	0.573
Top − 1	0.190	0.204	0.356	0.182	0.323	0.274
Middle	0.060	0.024	0.128	0.016	0.187	0.101
Bottom + 1	0.094	0.085	0.023	0.000	0.083	0.038
Bottommost	0.217	0.189	0.003	0.000	0.080	0.017
Surface state?	Yes	Yes	Yes	Yes	No	Yes

$\bar{M}_3$. Thus, the 1 and 2-QL slabs have topologically trivial ($\nu_0 = 0$) surface states. Let us discuss the slabs three or more QLs thick. Their surface states are marked in Figs. 2(c)–2(f). In the vicinity of E_F, only two surface bands are identified. The features of these two surface bands discussed below do not depend on the thickness. To better examine the surface states, for example, for the 5-QL slab, the projections of the wave function onto each QL at three $k_{\|}$ points for the two energy bands [shown in the inset of Fig. 2(e)] are listed in Table II. The v-shaped valence band near $\bar{\Gamma}$ is a surface band [Figs. 2(c)–2(f)]. This surface band intersects E_F only once between $\bar{\Gamma}$ and $\bar{M}$ [insets in Figs. 2(c) and 2(e)] and joins the bulk bands as $k_{\|}$ moves further away from $\bar{\Gamma}$. The occupied U-shaped band slightly below the v-shaped band near $\bar{\Gamma}$ [insets in Figs. 2(c) and 2(e)], is again a surface band only within a very narrow window in $k_{\|}$, yet it loses its surface character before it crosses E_F [see the projections of this band at the E point, E_{U}, in Table II and the inset of Fig. 2(e)]. Additionally, none of the surface bands cross E_F between $\bar{M}_2$ and $\bar{M}_3$. Thus, slabs three or more QLs thick have topologically nontrivial ($\nu_0 = 1$) surface states, independent of the thickness. Table II also implies that the decay length of the surface states is about 2 nm since the wave function projections significantly decrease beyond 2 QLs. Our findings clearly reveal that the topological nature of the surface states persists with decreasing thickness, which can play a crucial role in transport measurements. These results differ from previous calculations [19–21] due to a different treatment of slabs, as discussed earlier.

In conclusion, we have constructed a method to accurately identify topological surface states within DFT. Using this method, we have investigated the topological nature of the surface states in thin films of $Bi_2Te_3(111)$ using DFT. We have found that the topological nature of the surface states remains robust with the film thickness and that the surface states are topologically protected for films of three or more QLs. The method and our findings are applicable to thin films of other types of TI.

The authors thank T. Stanescu for discussions. K. P. was supported by NSF DMR-0804665, D. M. by U.S. DOE DE-FG05-92ER40677, J. J. H. by U.S. DOE DE-FG02-08ER46532. Computational support was provided by Intel 64 cluster (Abe) at the NCSA under DMR060009N and VT ARC.

[1] L. Fu and C. L. Kane, Phys. Rev. B **76**, 045302 (2007).
[2] J. C. Y. Teo, L. Fu, and C. L. Kane, Phys. Rev. B **78**, 045426 (2008).
[3] X.-L. Qi, T. L. Hughes, and S. C. Zhang, Phys. Rev. B **78**, 195424 (2008).
[4] M. Z. Hasan and C. L. Kane, arXiv:1002.3895v1 [Rev. Mod. Phys. (to be published)].
[5] H. Zhang *et al.*, Nature Phys. **5**, 438 (2009).
[6] D. Hsieh *et al.*, Nature (London) **452**, 970 (2008); D. Hsieh *et al.*, Science **323**, 919 (2009).
[7] Y. L. Chen *et al.*, Science **325**, 178 (2009).
[8] Y. Xia *et al.*, Nature Phys. **5**, 398 (2009).
[9] D. Hsieh *et al.*, Nature (London) **460**, 1101 (2009).
[10] K. K. Gomes *et al.*, arXiv:0909.0921.
[11] W. Zhang *et al.*, New J. Phys. **12**, 065013 (2010).
[12] P. Ghaemi *et al.*, Phys. Rev. Lett. **105**, 166603 (2010).
[13] T. Hirahara *et al.*, Phys. Rev. B **81**, 165422 (2010).
[14] G. Zhang *et al.*, Appl. Phys. Lett. **95**, 053114 (2009).
[15] Y. Zhang *et al.*, Nature Phys. **6**, 584 (2010).
[16] Y.-Y. Li *et al.*, arXiv:0912.5054.
[17] Y. Sakamoto *et al.*, Phys. Rev. B **81**, 165432 (2010).
[18] D. Teweldebrhan *et al.*, Appl. Phys. Lett. **96**, 053107 (2010); , Nano Lett. **10**, 1209 (2010).
[19] C.-X. Liu *et al.*, Phys. Rev. B **81**, 041307(R) (2010).
[20] J. Linder *et al.*, Phys. Rev. B **80**, 205410 (2009).
[21] H.-Z. Lu *et al.*, Phys. Rev. B **81**, 115407 (2010).
[22] S. K. Mishra *et al.*, J. Phys. Condens. Matter **9**, 461 (1997).
[23] S. Nakajima, J. Phys. Chem. Solids **24**, 479 (1963).
[24] G. Kresse and J. Furthmüller, Phys. Rev. B **54**, 11169 (1996); G. Kresse and J. Furthmüller, Comput. Mater. Sci. **6**, 15 (1996).
[25] J. P. Perdew, K. Burke, and M. Ernzerhof, Phys. Rev. Lett. **77**, 3865 (1996).
[26] P. E. Blöchl, Phys. Rev. B **50**, 17953 (1994).
[27] G. Wang and T. Cagin, Phys. Rev. B **76**, 075201 (2007).
[28] S. Cho *et al.*, Appl. Phys. A **79**, 1729 (2004).
[29] M. R. Thuler *et al.*, Chem. Phys. **71**, 265 (1982).
[30] S. V. Halilov *et al.*, Phys. Rev. B **52**, 14235 (1995).
[31] J. R. Smith, J. G. Gay, F. J. Arlinghaus, Phys. Rev. B **21**, 2201 (1980).
[32] J. Furthmüller, J. Hafner, and G. Kresse, Phys. Rev. B **53**, 7334 (1996).
[33] A. Euceda *et al.*, Phys. Rev. B **27**, 659 (1983).